Asian Journal of Pharmaceutical Sciences 15 (2020) 591–604

Available online at www.sciencedirect.com

ScienceDirect

journal homepage: www.elsevier.com/locate/AJPS

Original Research Paper

Development of novel cationic microemulsion as parenteral adjuvant for influenza vaccine

Sakalanunt Lamaisakul[a], *Angkana Tantituvanont*[a], *Vimolmas Lipipun*[b], *Garnpimol Ritthidej*[a,*]

[a] *Department of Pharmaceutics and Industrial Pharmacy, Faculty of Pharmaceutical Sciences, Chulalongkorn University, Bangkok 10330, Thailand*

[b] *Department of Biochemistry and Microbiology, Faculty of Pharmaceutical Sciences, Chulalongkorn University, Bangkok 10330, Thailand*

ARTICLE INFO

Article history:
Received 12 July 2018
Revised 25 July 2019
Accepted 8 August 2019
Available online 10 September 2019

Keywords:
Cationic microemulsion
Adjuvant
Influenza virus
Vaccine

ABSTRACT

Squalene-based oil-in-water (O/W) emulsions have been used as effective and safe adjuvants in approved influenza vaccines. However, there are concerns regarding the safety and side effects of increasing risk of narcolepsy. In present study, novel O/W microemulsions (MEs) containing wheat germ oil, D-alpha tocopheryl polyethylene glycol 1000 succinate (TPGS) and Cremophor EL (CreEL) or Solutol HS15 were formulated with/without a cationic surfactant, cetyltrimethylammonium bromide (CTAB) and then sterilized by autoclaving. Their physical properties and biological efficacies were evaluated. The results demonstrated that autoclaving reduced the droplet size to ~20 nm with narrow size distributions resulting in monodisperse systems with good stability up to 3 years. Hemolytic activity, viscosity, pH, and osmolality were appropriate for parenteral use. Bovine serum albumin (BSA), a model antigen, after mixing with MEs retained the protein integrity, assessed by SDS-PAGE and CD spectroscopy. Greater percentages of 28SC cell viability were observed from CreEL-based MEs. Uptake of FITC-BSA-MEs increased with the increasing concentration of CTAB confirmed by CLSM images. Furthermore, cationic CreEL-based MEs could induce Th1 cytokine synthesis with an increase in TNF-α and IL-12 levels and a decrease in IL-10 level. *In vivo* immunization study in mice of adjuvants admixed with influenza virus solution revealed that nonionic and selected cationic CreEL-MEs enhanced immune responses as measured by influenza-specific serum antibody titers and hemagglutination inhibition titers. Particularly, cationic CreEL-based ME showed better humoral and cellular immunity with higher IgG2a titer than nonionic CreEL-based ME and antigen alone. No differences in immune responses were observed between mice immunized with selected cationic CreEL-based ME and marketed adjuvant. In addition, the selected ME induced antigen-sparing while retained immune stimulating effects compared to antigen alone. No inflammatory change in muscle fiber structure was observed. Accordingly, the developed cationic CreEL-based ME had potential as novel adjuvant for parenteral influenza vaccine.

* Corresponding author. Department of Pharmaceutics and Industrial Pharmacy, Faculty of Pharmaceutical Sciences, Chulalongkorn University, Phayathai Road, Patumwan District, Bangkok 10330, Thailand. Tel.:+662 218 8273
E-mail address: garnpimol.r@chula.ac.th (G. Ritthidej).
Peer review under responsibility of Shenyang Pharmaceutical University.

https://doi.org/10.1016/j.ajps.2019.08.002

1. Introduction

Prophylactic vaccination has been the most effective method to prevent influenza virus infections which cause considerable mortality and morbidity worldwide each year. New influenza vaccine has to be annually produced to match the predicted predominant circulating strains of the next season following WHO recommendation. Consequently, novel adjuvants have been sought despite the effective and approved squalene-based O/W nanoemulsions partially regarding to the side effects and safety of squalene from shark on the increasing risk of narcolepsy even though the trigger for this sleep-related adverse event is not yet clarified [1]. In addition, the chemical surfactants of polysorbate and sorbitan oleate in MF59™ adjuvant as well as polysorbate 80 and α-tocopherol in AS03 adjuvants remain contentious for intramuscular injection [2]. Thus, more powerful and safer emulsion adjuvants for influenza vaccine have been intensively developed such as emulsion of the combined Alhydrogel ($Al(OH)_3$) with monophosphoryl lipid A [3], microemulsion (ME) of dioctadecyldimethylammonium bromide and a mineral oil [4], soybean O/W nanoemulsion [5], O/W emulsion containing squalene, egg lecithin and sodium oleate [6] and O/W emulsion of gum arabic and mineral oil [7].

ME, a novel vehicle for parenteral drug delivery system to improve target specificity and therapeutic activity has superior advantages of spontaneous formation and thermodynamic stability over nanoemulsion [8]. It has been explored as an alternative adjuvant for influenza vaccine [4] including to improve immune-enhancing activity of a flavonoid [9] and as an intranasal adjuvant [10]. No local reactions were exhibited from ME formulation of isopropyl myristate, polysorbate 80 and propylene glycol as adjuvants for rabies virus [11] and bluetongue vaccine [12]. This ME formulation was the best candidate for rabies vaccine while showed low antibodies titer for bluetongue vaccine likely due to the difference in the final particle size since the adjuvanticity of systems was reported to be mediated by the average particle size. Particle size of 20–50 nm resulted in maximum cellular uptake [13] and more readily taken up into the lymphatic system and more efficiently induced the lymph node-resident dendritic cells [14].

As an animal-friendly alternative, wheat germ oil, a compound listed in European compendium contains low squalene content. However, the cold-pressed wheat germ oil has the highest content of vitamin E which can help to achieve the highest antibody response [15]. In addition, infusion of wheat germ oil formulated as nanoemulsion showed no cytotoxicity in both vero and HaCaT cells at a concentration of 100 µg/ml [16]. This vegetable oil was used in parenteral emulsion of cinobufagin, a compound with immunomodulatory effects [17]. Moreover, W/O emulsion vaccines for Newcastle disease containing wheat germ oil showed light tissue reaction compared to other vegetable oils [18].

Emulsifier, an essential component for spontaneous ME formation, is generally used in high concentration with/without co-emulsifier. Cremophor EL (CreEL, Polyoxyl 35 castor oil) and Solutol HS15 (Macrogol 15 hydroxystearate) are nonionic surfactants that have been recognized as safe and have been used for parenteral administration in high concentrations up to 50%–65%. D-alpha tocopheryl polyethylene glycol 1000 succinate (TPGS), an approved pharmaceutical adjuvant is a vitamin E derived emulsifier. Despite a weak emulsifier, the presence of TPGS could improve the antibody responses in oral vaccine preparations for *Vibrio anguillarum* O2 antigen [19] and for diphtheria toxoid by intranasal administration [20].

Cell association between vaccine delivery system or antigen and antigen presenting cells is an important step to stimulate immunogenicity. Thus the physicochemical properties of the formers including composition and particle surface characteristics accordingly affect the immune cell association. The uptake of liposomes by murine bone marrow macrophages was influenced by liposome composition [21] while charged delivery systems are preferably phagocytosed by immune cells [22]. In addition, modification of PLGA microparticles with cetyltrimethylammonium bromide (CTAB), a cationic surfactant increased *in vitro* cellular uptake and internalization of antigen [23] and stimulated the production of Th1-type cytokines [24].

This study was therefore aimed to develop ME formulation as an alternative adjuvant for parenteral influenza vaccines. Nonionic surfactants of CreEL, Solutol HS15, and TPGS were to stabilize the wheat germ oil in novel O/W ME formulations, with the absence and presence of cationic surfactant, CTAB. Physical properties and hemolysis activity of the developed ME adjuvants were evaluated. Integrity of bovine serum albumin (BSA) as a model antigen and its in-vitro biological properties in human monocyte/macrophage cells were also investigated. Finally, the developed ME adjuvants admixed with influenza antigen were immunized in mice model and their biological properties including the safety and adjuvanticity were assessed and compared with a commercial squalene-based emulsion adjuvant.

2. Materials and methods

2.1. Materials

Wheat germ oil, bovine serum albumin (BSA) (lyophilized powder, Cohn Fraction V albumin), fluorescein isothiocyanate conjugate bovine (FITC-BSA), poly-L-lysine, and Fluoroshield™ with DAPI histology mounting medium were purchased from Sigma-Aldrich, St' Louis, MO, USA. Polyoxyl 35 castor oil (Cremophor® EL (CreEL)), Macrogol 15 hydroxystearate (Solutol® HS15), and D-alpha tocopheryl polyethylene glycol 1000 succinate (TPGS) (Speziol® TPGS Pharma) were from BASF Corp. Ludwigshafen, Germany. Cetyltrimethylammonium bromide (CTAB), molecular biology grade, Calbiochem®, Merck KGaA was obtained from Merck Millipore Corp., Darmstadt, Germany. Human monocyte/macrophage cells (28SC, ATCC® CRL 9855TM) was from American Type Culture Collection, Manassas, VA, USA. Iscove's Modified Dulbecco's Medium (IMDM) (1X) + 4 mM L-Glutamine + 25 mM HEPES, HT Supplement

(100X) (10 mM Sodium hypoxanthine and 1.6 mM Thymidine), 2-Mercaptoethanol, Fetal Bovine Serum (FBS) and Hanks' Balanced Salt Solution (HBSS) (1X) were from Gibco Invitrogen, NY, USA. Alamar Blue® reagent was purchased from Invitrogen, Frederick, MD, USA. Commercial squalene-based emulsion adjuvant was bought from InvivoGen, San Diego, CA92121, USA. Alexa Fluor 594-wheat germ agglutinin (WGA) was obtained from Life Technologies, Eugene, OR, USA. Receptor-destroying enzyme (RDE) II was procured from Denka Seiken, Tokyo, Japan. Human tumor necrosis factor-alpha (TNF-α) Instant ELISA was from eBioscience, USA. Interleukin-12 (IL-12) p70, interleukin-10 (IL-10) Human ELISA Kit tests, and horseradish peroxidase-conjugated goat anti-mouse IgG, IgG1, and IgG2a antibodies were purchased from Abcam, UK. Influenza vaccine was kindly provided from Government Pharmaceutical Organization, Thailand. Other chemicals are analytical grade.

2.2. Construction of pseudoternary phase diagrams

Pseudoternary phase diagrams were constructed by using water titration technique to define the regions of ME formation. CreEL and Solutol HS15 were blended with TPGS in different mass ratios (Km) at 1:3, 1:1, and 3:1 of TPGS to CreEL or TPGS to Solutol HS15. The mixtures of 9:1 to 1:9 wt ratios of wheat germ oil and the nonionic surfactant blend were then heated on a water bath at 45°C until TPGS was completely melted. Each mixture was serially titrated with water at ambient temperature, mixed and vortexed thoroughly for 20 s to equilibrate the system. ME was marked as shade areas in each pseudoternary phase diagram when the appearance was transparent or translucent and flowable.

2.3. Preparation of me adjuvants

Wheat germ oil at concentration of 5% (w/w) was selected according to the oil phase concentration of commercial squalene-based emulsion adjuvant. In order to optimize the concentration of total nonionic surfactants for the production of O/W MEs, different concentrations of total nonionic surfactants from ME region on phase diagrams at high water content were prepared for formulation screening. Each mixture of oil and surfactant blend was melted on a water bath at 45°C, then mixed with ultrapure water or a solution containing 0.2%, 0.4% and 0.6% (w/v) CTAB at room temperature. The developed adjuvant formulations were sterilized by autoclaving (Hiclave^{TM}, HVE-50, Hirayama, Japan) for 20 min at 121°C, 15 psi, and stored by refrigeration at 2–8°C. The ME formulations were designated by codes as C0, C2, C4, and C6 for CreEL-based MEs and S0, S2, S4, and S6 for Solutol HS15-based MEs containing 0, 0.2%, 0.4% and 0.6% (w/v) CTAB, respectively. A commercial squalene-based emulsion adjuvant used for comparison was designated as M.

2.4. Characterization of adjuvant formulations

2.4.1. Particle size and polydispersity measurements

Before and after autoclaving, the particle size and polydispersity of the obtained MEs were evaluated by dynamic light scattering (DLS) technique with a Zetasizer Nano-ZS (Malvern Instruments, UK). Prior to evaluation, equal volumes of each formulation and PBS pH 7.4 were mixed. This sample dilution factor is according to the mixture of the marketed adjuvant with equal volume of antigen prior to administration. The analysis was performed in triplicate at 25°C.

2.4.2. Zeta potential determination

Each ME sample was diluted 1:1 volume ratio with ultrapure water prior to Zeta potential measurements on the Zetasizer Nano-ZS (Malvern Instruments, UK). The measurements were evaluated in triplicate at 25°C.

2.4.3. Determinations of viscosity, pH and osmolality

A Vibro viscometer (Model SV-10 series, A&D Company Limited, Japan) was used to determine the dynamic viscosities of samples before and after autoclaving. The average viscosity values were calculated from triplicate and demonstrated as milli-pascal-second (mPa.s). The pH values of samples before and after autoclaving were assessed in triplicate using a pH meter (FE20 FiveEasyTM, Mettler Toledo, USA) whereas the osmolalities of the obtained MEs were determined by using an osmometer (Osmomat 030-D Automatic cryoscopic osmometer, Gonotec, Germany).

2.5. Hemolysis study

The *in vitro* hemolysis procedure from a previous report was followed [25]. Human whole heparinized blood from the Thai Red Cross Society was stored at 5 °C and used within a week of collection. In general, hemolysis activity was reported as a percentage normalized to the positive control (100% lysis) and assessed on blood samples from three different donors for each sample with triplicated repeats. The hemolysis% was calculated by the following Eq. 1.

$$\text{Hemolysis\%} = 100 \times (\text{Abs} - \text{Abs}_0)/(\text{Abs}_{100} - \text{Abs}_0) \quad (1)$$

Where Abs, Abs_0 and Abs_{100} were absorbance measurements of treated red blood cell (RBC) suspension incubated with the adjuvant formulations, normal saline (negative control) and distilled water (positive control), respectively.

2.6. Stability study of me formulation

The MEs were stored at 2–8 °C in a refrigerator for 3 years. The systems were then visually inspected for clarity or homogeneity. The particle size and polydispersity index were also determined following the procedure in 2.4.

2.7. Preparation of BSA-loaded formulations

The stock solution of BSA was first diluted by PBS pH 7.4 to a concentration of 30 µg/100 µl, and then was simply mixed 1:1 by volume with different sterile adjuvant formulations (BSA-MEs) including a commercial adjuvant (BSA-M) to obtain final concentration of BSA in preparation of 15 µg/100 µl.

2.8. Characterization of BSA-loaded formulations

Particle size, polydispersity, zeta potential, viscosity, pH, and osmolality of BSA-MEs were determined as described in Section 2.4 without further sample dilution and compared to corresponding ME formulations without BSA.

2.9. Studies on protein property

2.9.1. Sodium dodecyl sulfate-polyacrylamide gel electrophoresis (SDS-PAGE)

The BSA-MEs were mixed with NuPAGE® LDS Sample Buffer (4X), NuPAGE® Sample Reducing Agent (10X) and deionized water, resulting protein amount of 600 ng in each sample. The mixture samples were heated in boiling water for 10 min and cooled to room temperature before loading on to NuPAGE 4%–12% Bis-Tris Gel 1.0 mm with NuPAGE® MES SDS Running Buffer. The voltage was set at 200 V constant with 700 mA for 30 min. After electrophoresis, the protein bands were stained with SimplyBlueTM SafeStain and de-stained with deionized water until a clear background was obtained. The fragmentation of protein was compared with protein marker (SeeBlue® Plus2 Prestained Standard).

2.9.2. Circular dichroism (CD) measurements

Protein integrity of BSA in MEs was measured on CD compared with native BSA in PBS pH 7.4 as a control. CD spectra were determined with a Jasco J-715 spectropolarimeter (Jasco, Japan) using a 10 mm pathlength of rectangular quartz cell at 1.0 nm of resolution, 1.0 nm of bandwidth, 100 mDeg of sensitivity, and 100 nm/min of scan rate with five scans averaged for each CD spectrum. In addition, ellipticity (θ, mDeg) of each sample was reported by scanning in the range of 200–250 nm (far-UV region) at room temperature under continuous nitrogen purge. Each diluted adjuvant formulation without BSA as blank was subtracted from the individual sample spectrum as well as PBS pH 7.4 was run as background. The CD spectra were shown by plotting ellipticity against wavelength.

2.10. In vitro cell studies

2.10.1. Culturing of 28SC cells

The 28SC cells (ATCC® CRL 9855TM) originated from human peripheral blood mononuclear cells were grown in a horizontal plastic culture flask. Briefly, cells were maintained in IMDM (1X) + 4 mM L-Glutamine + 25 mM HEPES supplemented with 0.05 mM 2-mercaptoethanol, 0.1 mM hypoxanthine, 0.016 mM thymidine and fetal bovine serum to a final concentration of 10% as complete growth medium and incubated at 37 °C in a humidified 5% CO_2 incubator in air atmosphere. The cells grew as single cells in suspension, and have a granular appearance. These cells were split into 96-well plates for cytotoxicity study and 6-well plates for cellular uptake study, internalization study and cytokine assay.

2.10.2. Cytotoxicity study

The cell viability was tested by Alamar Blue assay. The 28SC cells were diluted in complete growth medium to a density of 1×10^5 cells/ml and cultured in 96-well plate, 100 µl/well. To determine appropriate volume not to exceed the allowance for a mouse per site of intramuscular injection, 25 and 50 µl of BSA-ME containing BSA 15 µg/100 µl were added in wells and incubated with the cells for 2 h in a humidified atmosphere at 37 °C and 5% CO_2. The Alamar Blue® reagent was added to each well containing 12.5 or 15 µl of Alamar Blue® per well (10%, v/v final concentration in the wells). Measurement of fluorescence development was executed with a microplate reader (VICTOR^3, Perkin Elmer, USA) after 24 h of incubation with Alamar Blue® at 560 nm excitation wavelength and 590 nm emission wavelength. The relative cell viability was demonstrated as a percentage relative to the control group.

2.10.3. Cellular uptake study

Immune cells were cultured in 6-well plate at a density of 1×10^6 cells/ml in each well. FITC-BSA in PBS pH 7.4 incorporated with each ME was incubated for 2 h at 37 °C. Samples contained FITC-BSA 15 µg/100 µl. After incubation, the cells were centrifuged at 1500 rpm for 5 min and washed 3 times with cold PBS to eliminate non-internalized FITC-BSA bound to the cell surface and to decrease the extracellular fluorescence and resuspended in PBS pH 7.4. Fluorescein uptake was measured by fluorescence-assisted cell sorter (FACS, BD-FACSalibur, Becton Dickinson, USA) equipped with an argon laser and detected with a G1 detector (excitation of 485 nm and emission of 525 nm). The data were calculated by using the instrument software and the degree of FITC-BSA uptake was shown as the geometric mean fluorescence intensity (GeoMFI) ± SD and performed in triplicate.

2.10.4. Cytokine assay

Cytokines in cell culture supernatant were determined using TNF-α, IL-12 p70 (70-kDa), and IL-10 sandwich ELISA sets, following the manufacturer's instructions. Cell culture medium of incubated 28SC cells with 25 µl of each BSA-loaded ME formulation for 24 h in humidified atmosphere (5% CO_2, 37 °C) was centrifuged at 1500 rpm for 5 min and stored at −20 °C until quantification of the cytokine level.

2.10.5. Internalization study

Intracellular localization of FITC-BSA (green) into human immune cells was investigated by a FluoView FV10i-DOC confocal laser scanning microscope (CLSM, Olympus, Tokyo, Japan). Immune cells were adhered to 0.01% poly-L-lysine coated coverslips, incubated for 2 h at 37 °C in the presence of FITC-BSA in each sample and washed three times with PBS. Then attached cells were incubated with 5 µg/ml of Alexa Fluor 594-wheat germ agglutinin (WGA) in HBSS for 10 min at 37 °C to stain plasma membrane and visualize the cell boundary, washed twice with HBSS. The cells then were fixed with 4% formaldehyde solution in PBS for 15 min at room temperature and rewashed twice with PBS. Each slide was mounted by a single drop of Fluoroshield™ with DAPI histology mounting medium for nuclear staining, and then the edges of the coverslip were sealed with clear nail polish for visualization by using CLSM.

2.11. Preparation of antigen-loaded formulations for immunization

Influenza vaccine composed of monovalent bulk of IIV, Influenza A (H1N1) Virus (inactivated, split), strain A/H1N1/California/07/2009 was used as vaccine antigen. Stable formulations with safety and efficacy from the *in vitro* cellular results, thus potentially great adjuvanticity were selected to be tested in animal studies. The inoculation mixtures were prepared aseptically under a laminar flow cabinet to minimize contamination. Briefly, the antigen solution was mixed with PBS (antigen alone), marketed adjuvant (Ag-M) or selected MEs in a 1:1 volume ratio to obtain the concentration of antigen of 5 μg/50 μl per dose prior to intramuscular injection. To evaluate the antigen-sparing effect of ME formulation, antigen was diluted appropriately with PBS and mixed with an equal volume of a selected ME to obtain a final vaccine preparation containing half-dose antigen (2.5 μg/50 μl).

2.12. Animals immunization

Female, 7 weeks old, BALB/c mice (National Laboratory Animal Center, Mahidol University, Thailand), were housed in groups of eight mice and maintained in the animal facility of Chulalongkorn University Laboratory Animal Center (CU-LAC) with a 12 h day and night schedule, while food and water were *ad libitum*. The experiments were approved by the Ethical Committee for Animal Experimentation of Chulalongkorn University, protocol number 1 573 011.

Six groups of BALB/c mice were intramuscularly vaccinated two times at 3-week interval (0 and 21 d) with either influenza vaccine antigen alone or in combination with adjuvant by injection into the gastrocnemius muscles in the two hind legs with 25 μl/leg (50 μl total per mouse). The blood samples of individual mice were taken from submandibular vein before and 3 weeks following the first and second immunizations. At the end of the experiment, mice were sacrificed by using carbon dioxide inhalation prior to cervical dislocation and collect the blood from cardiac puncture. Individual blood samples were centrifuged for 10 min at 4000 rpm at 4°C, and then serum samples were separated from blood cells and coagulated proteins and stored at −20°C till the day of analysis.

2.13. Antibody assessment

For determination of the influenza virus-specific antibody responses, the enzyme-linked immunosorbent assay (ELISA) was conducted [6]. Briefly, high-affinity EIA/RIA 96 well plates (#3590, Corning®, NY, USA) were coated with of 200 ng/100 μl dilution of influenza vaccine (H1N1) per well in bicarbonate coating buffer (0.05 M carbonate-bicarbonate, pH 9.6) and incubated overnight at 37 °C. Plates were thoroughly washed 3 times with 300 μl of washing buffer (PBS containing 0.05% (v/v) Tween 20, PBST, pH 7.4) per well and then blocked by incubation with 150 μl of 1% (w/v) BSA in PBS pH 7.4 at 37 °C for 1 h prior to washing 3 times with PBST. Appropriate serial dilutions of the sample with diluting buffer (PBS containing 0.05%, v/v 56 °C Tween 20 and 0.1%, 37 °C w/v BSA) of each individual mouse were added to the plates and incubated for 2 h at 37 °C. After washing three times with PBST, 100 μl horseradish peroxidase-conjugated goat anti-mouse IgG, IgG1, and IgG2a antibodies were added at a 1:10 000 dilution and incubated for 1 h at 37 °C. After washing as above, color reaction was developed by adding 3,3′,5,5′-tetramethylbenzidine (TMB) solution, 100 μl per well. The plates were placed in the dark for 15 min at room temperature. Then the enzymatic reaction was stopped by adding 50 μl of 1.0 N H_2SO_4 as stop reagent and the optical densities (OD) were measured at 450 nm using microplate reader (VICTOR3, Perkin Elmer, USA) within 5 min. Antibody titers were expressed as the highest dilution having a mean OD value that was greater than the mean value plus three times the standard deviations of the average OD obtained in the pre-immune serum samples. Comparison of antibody titers between groups was made by a one-way ANOVA program.

2.14. Hemagglutination inhibition assay

2.14.1. Hemagglutinin (HA) titer determination

Briefly, 50 μl of two-fold serially diluted antigens (Influenza A (H1N1) virus (inactivated, whole virus), strain A/H1N1/California/07/2009) in PBS were added to an equal volume of 0.5% goose RBC suspension in 96-well microplate V-bottom. Following 30 min incubation at room temperature (22–25 °C) or settling of RBC control wells, the plates were then tilted at approximately a 60° angle and wells read for hemagglutination defined as a diffuse pattern of settling on the well bottom. HA titer was determined to be the reciprocal of the highest virus dilution exhibiting the settled complete hemagglutination. The antigen dilution was then calculated and prepared to 4 hemagglutination units (HAU) of antigen in 25 μl.

2.14.2. Hemagglutinin inhibition (HAI) titer determination

HAI antibody titers were determined using sera collected 3 weeks after the first and second immunizations of antigen alone or adjuvant vaccines. HAI antibody specific to the H1N1 influenza virus was determined as previously described [26] using 0.5% goose RBC suspension. Individual serum samples were pre-treated with three parts receptor-destroying enzyme (RDE) II by incubation overnight at 37 °C to eliminate non-specific anti-hemagglutination activity existing in serum samples followed by heating at 56 °C for 45 min to deactivate the residual cholera activity. After cooling to room temperature, each pretreated serum was added 6 parts of PBS with a starting serum dilution of 1:10 for the assay in the first well. Subsequently, 25 μl of serial 1:2 diluted samples into PBS in V-bottom microtiter plates were mixed with 25 μl of influenza antigen and incubated at room temperature for 30 min. The mixtures were then added to an equal volume of 0.5% goose RBC suspension in 96-well microplate V-bottom and incubated again for 30 min or settling of RBC control wells as a negative control. All individual serums were run in duplicate. The HAI titer is defined as the serum dilution in which the last complete agglutination inhibition occurs by tilting the plates

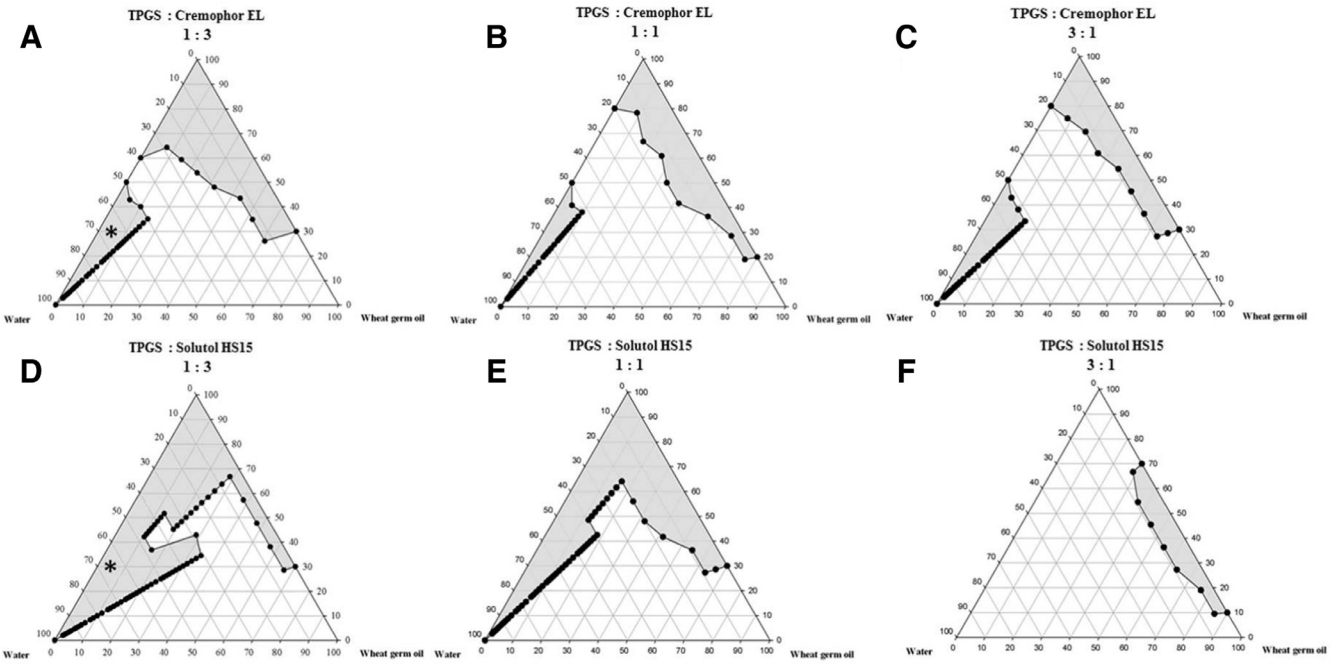

Fig. 1 – Schematic pseudoternary phase diagrams of wheat germ oil and water at 1:3, 1:1 and 3:1 (w/w) ratio of D-alpha tocopheryl polyethylene glycol 1000 succinate (TPGS) and (A-C) Cremophor® EL (CreEL) or (D-F) Solutol HS15 as surfactants, respectively, showing the existence of ME region in the gray area in which each asterisk * represents the optimal ratio of the ME compositions used in this study.

at approximately a 60° angle and presence of tear-shaped streaming of RBCs which flow at the same rate as RBC controls. The antibody concentration corresponds to the reciprocal value of the titer. The geometric mean titers (GMT) of eight mice per group are shown.

2.15. *Histomicroscopic examinations*

Three weeks after the last immunization, the mice were sacrificed and the gastrocnemius muscles at behind legs from immunized mice were removed and performed by the histomicroscopic study. The muscles were immediately fixed in 10% neutral buffered formalin, embedded in paraffin wax, and processed by the routine technique of standard procedures. Histological sections were stained with hematoxylin and eosin (H&E) and observed using a digital slide scanner (Pannoramic SCAN 1.12, 3DHISTECH, Ltd., Budapest, Hungary) and image capture software (CaseViewer 1.4 Software, 3DHISTECH, Ltd., Budapest, Hungary).

2.16. *Statistical analysis*

Data were presented as the mean ± SD values. The differences among each treatment group were assessed by the simple analysis of variance (one-way ANOVA) followed by multiple comparison post-hoc tests using Turkey's and Dunnett's T3 pairwise comparisons, if there was or was not homogeneity of variance, respectively. All analysis was statistically calculated using IBM® SPSS® statistics version 21 and significant differences were considered at a level of $P<0.05$.

3. Results and discussion

3.1. *Pseudoternary phase diagrams*

Each vertex in the triangle pseudoternary phase diagram represents 100% wheat germ oil, 100% total surfactant, and 100% water phase, respectively. The shaded areas of pseudoternary phase diagrams represented the boundary of ME region. Comparison between the ME regions of systems containing TPGS and CreEL surfactant mixture and TPGS and Solutol HS15 surfactant mixture in different mass ratios (Km) at 1:1, 1:3, and 3:1, respectively (Fig. 1) revealed that higher amount of CreEL or Solutol HS15 in the surfactant mixture at the Km of 1:3 provided larger shaded area of ME than at Km of 1:1 and 3:1, respectively. Both CreEL and Solutol HS15 had an influence on the expansion region of the ME, likely by increasing the interfacial fluidity via intercalation and entanglement with TPGS surfactant film. Thus, TPGS to CreEL and TPGS to Solutol HS15 at the Km of 1:3 were selected. Moreover, system with lower amounts of surfactants was preferred due to less cytotoxicity. ME composition containing 5% wheat germ oil, 30% total nonionic surfactants, and water q.s. to 100% was optimal and marked by each asterisk (*) (Fig. 1A and 1B) to which different concentrations of CTAB were then incorporated.

3.2. ME characterization

The characteristics of all prepared MEs, both before and after autoclaving are summarized in Table 1 while those of BSA-MEs are listed in Table 2.

3.2.1. Particle size and polydispersity measurements

Prior to autoclaving, the mean droplet size of C0 was about 120 nm similar to that of M while that of the S0 was much smaller of about 25 nm (Table 1). This was likely due to the more complex structure of CreEL than Solutol HS15 to completely cover the droplet interface. The addition of CTAB obviously increased the mean droplet size of CreEL-based ME but moderately in Solutol HS15-based ME. At the highest concentration of CTAB added, the size increment was less in CreEL-based ME but substantial in Solutol HS15-based ME. All MEs had high polydispersity values (0.48–0.96) indicating of polydisperse systems. However, after autoclaving, the droplet size was decreased to about 20 nm with narrow size distributions resulting in monodisperse systems. A contrast result of increasing droplet size and polydispersity index after autoclaving had been reported [8]. This could be explained on the basis of cloud point. Dehydration of surfactant at temperatures above the cloud point could cause a breakdown of the film around the oil droplets. Surfactants rapidly relocated from aqueous to oily phase and rearranged at the interface during autoclaving [27]. Since smaller droplets needed more surfactant for stabilization than larger ones, the rearrangement of high concentration surfactant during heat sterilization would thus cause a decrease in droplet size and PI.

Upon loading with BSA solution, a slight increase in droplet size of BSA-MEs was obtained (Table 2). The deposition of BSA occurred at the interface of aqueous and oil droplets that the hydrophilic and hydrophobic residues interacted with water and the oil phase, respectively.

3.2.2. Zeta potential determination

Both zeta potential of C0 and S0 were of negative values (Table 1). Incorporation of CTAB gradually elevated the zeta potential to positive values due to increasing of the masking effect of cationic surfactant layer on the surface of lipid droplets. After autoclaving, the zeta potential slightly decreased from the increased concentration of free fatty acid during autoclaving. The incorporation of BSA solution in ME formulations led to a slight increase in zeta potential values (Table 2). This was the result of the net charge of BSA protein that changed to be positive at the acidic condition.

3.2.3. Viscosity measurements

C0 and S0 had different viscosity values of 129.00 and 25.43 mPa.s, respectively due to higher viscosity of CreEL (1010 mPa.s) than Solutol HS15 (428 mPa.s). Addition of CTAB solution especially at high concentration as well as autoclaving seemed to increase the viscosity value. The viscosity values of BSA-MEs were around 3.55 to 4.65 mPa.s (Table 1) and were close to those of water (~1 centipoise) indicating of ease upon intramuscular administration.

Table 1 – Physical properties and hemolysis activity of ME formulations (mean ± SD, $n = 3$).

Formulations*	Size (nm)[a]		PI[a]		Zeta potential (mV)[b]		Viscosity (mPa.s)		pH		Osmolality (mOsmol/kg)	Hemolysis(%)
	BA	AA	BA	AA	BA	AA	BA	AA	BA	AA		
C0	120.50 ± 15.70	17.40 ± 0.14	0.68 ± 0.07	0.24 ± 0.01	−14.53 ± 3.81	−12.10 ± 1.11	129.00 ± 0.00	115.00 ± 0.00	–	4.85 ± 0.01	458.3 ± 3.8	0.05 ± 0.17
C2	570.87 ± 24.99	17.33 ± 0.02	0.62 ± 0.02	0.25 ± 0.00	0.43 ± 0.49	−0.31 ± 0.35	157.33 ± 0.58	170.00 ± 1.00	5.23 ± 0.07	4.56 ± 0.01	457.7 ± 12.1	−0.03 ± 0.11
C4	235.67 ± 11.91	17.14 ± 0.39	0.92 ± 0.09	0.31 ± 0.01	2.82 ± 0.76	1.92 ± 0.53	198.67 ± 0.58	211.00 ± 2.00	4.98 ± 0.03	4.53 ± 0.02	471.7 ± 7.0	0.03 ± 0.05
C6	62.07 ± 8.50	–	0.93 ± 0.09	–	2.94 ± 1.38	–	–	–	–	–	514.3 ± 21.7	2.80 ± 0.70
S0	25.80 ± 0.06	22.52 ± 0.15	0.41 ± 0.06	0.32 ± 0.03	−7.99 ± 4.05	−1.03 ± 0.34	25.43 ± 0.06	28.93 ± 0.06	4.36 ± 0.00	4.51 ± 0.01	762.7 ± 8.3	0.19 ± 0.25
S2	49.82 ± 0.14	19.63 ± 0.07	1.00 ± 0.00	0.20 ± 0.03	0.95 ± 0.11	1.55 ± 1.05	23.97 ± 0.06	24.67 ± 0.12	4.23 ± 0.01	4.15 ± 0.01	805.3 ± 12.3	0.14 ± 0.10
S4	59.90 ± 0.78	20.12 ± 0.04	1.00 ± 0.00	0.23 ± 0.01	4.48 ± 0.89	3.06 ± 1.66	34.23 ± 0.15	34.97 ± 0.15	4.32 ± 0.02	4.04 ± 0.01	841.0 ± 34.7	0.24 ± 0.35
S6	542.20 ± 21.72	–	0.80 ± 0.11	–	5.66 ± 0.18	–	–	–	–	–	–	–
M	117.23 ± 1.76	–	0.20 ± 0.02	–	−1.29 ± 1.58	–	1.39 ± 0.01	–	6.69 ± 0.05	–	36.3 ± 0.6	−0.09 ± 0.11

* C and S represent CreEL-based MEs and Solutol HS15-based MEs and the numbers of 0, 2, 4 and 6 are 0, 0.2%, 0.4% and 0.6% (w/v) CTAB in formulations, respectively.

[a] Diluted each formulation with PBS in 1:1 ratio.

[b] Diluted each formulation with ultrapure water in 1:1 ratio.

Abbreviations: PI, Polydispersity index; BA, Before autoclaving; AA, After autoclaving; M, Marketed product.

Table 2 – Physical properties of BSA-loaded formulations (mean ± SD, $n = 3$).

Formulations*	Size (nm)	PI	Zeta potential (mV)	Viscosity (mPa.s)	pH	Osmolality (mOsmol/kg)
BSA-PBS	–	–	–	1.38 ± 0.01	7.42 ± 0.02	302.7 ± 1.2
BSA-C0	18.03 ± 0.09	0.26 ± 0.00-	−4.22 ± 3.71	4.13 ± 0.02	6.34 ± 0.01	263.3 ± 3.1
BSA-C2	19.09 ± 0.16	0.31 ± 0.03	0.91 ± 3.93	4.59 ± 0.01	6.07 ± 0.01	267.0 ± 1.0
BSA-C4	17.43 ± 0.25	0.26 ± 0.00	1.91 ± 0.61	4.65 ± 0.02	5.90 ± 0.01	273.0 ± 3.0
BSA-S0	21.35 ± 0.34	0.20 ± 0.02	−0.93 ± 0.61	3.85 ± 0.02	5.54 ± 0.01	346.0 ± 3.0
BSA-S2	19.71 ± 0.26	0.21 ± 0.02	1.02 ± 1.49	3.55 ± 0.02	5.42 ± 0.00	346.3 ± 5.5
BSA-S4	20.13 ± 0.18	0.21 ± 0.00	3.44 ± 2.96	3.70 ± 0.01	5.19 ± 0.01	355.7 ± 3.5
BSA-M	119.63 ± 0.71	0.20 ± 0.02	1.64 ± 1.71	1.39 ± 0.03	6.99 ± 0.02	172.3 ± 0.6

* C and S represent CreEL-based MEs and Solutol HS15-based MEs and the numbers of 0, 2, 4 and 6 are 0, 0.2%, 0.4% and 0.6% (w/v) CTAB in formulations, respectively.
Abbreviations: PI, Polydispersity index; M, Marketed product.

3.2.4. *pH measurements*

All MEs were slightly acidic. Solutol HS15-based MEs had slightly higher acidity than CreEL-based MEs due to slightly lower pH value of Solutol HS15 solution (pH 6–7) than that of CreEL solution (pH 6–8) [28]. A slight decrease in pH was noted in all MEs upon autoclaving due to the stimulation of oil hydrolysis and degradation of the phospholipid emulsifier to create free fatty acids, thereby lowering pH of the unbuffered emulsion system. The addition of CTAB solution in MEs seemed to have no effect on pH value because of low amount of CTAB. Dilution with BSA solution in PBS pH 7.4 adjusted the pH of BSA-MEs closer to the acceptable physiologic pH range of about 5.0–9.0 implying of no cellular damage or phlebitis when administered parenterally (Table 2).

3.2.5. *Osmolality measurements*

All MEs had high osmolality value (457.67 to 471.67 mOsmol/kg for CreEL-based MEs formulations and 762.67–841.00 mOsmol/kg for Solutol HS15-based MEs) which depended on the number of moles of chemical compound in a solution. At equal mass of surfactant, CreEL which has higher molecular weight (2560 g/mol) had lower number of CreEL moles than those of Solutol HS15 which has molecular weight of 344 g/mol. Consequently, adding higher CTAB concentrations in formulation increased the osmolality values. Upon 1:1 diluting with BSA solution which had much lower osmolality value of 302.7 mOsmol/kg, these osmolality values were sharply reduced in BSA-MEs to 263–356 mOsmol/kg which were closer to the osmolality of PBS. The marketed adjuvant had the lowest osmolality of 172.3 mOsmol/kg. However, impact of osmolality on pain and burning sensation following intramuscular administration has not been reported.

3.3. *Stability studies of me formulation*

The physical instability of ME systems is indicated by changes in the droplet size and PI. The droplet sizes of the prepared MEs at initial were about 17.43–21.35 nm. After 3-year storage in a refrigerator, the sizes were 18.89–20.47 nm revealing less than 1.5 nm in size difference. There was no sign of phase separation and turbidity indicating of excellent stability.

3.4. *Hemolytic activity*

The prepared MEs showed very low hemolytic activity (Table 1). Nonionic surfactants with bulky chemical structure, various alkyl chains, high HLB, or more molecular mass has low hemolytic potency because of their low ability to penetrate into the lipid layer of RBC membranes [29]. In addition, CreEL and Solutol HS15 could protect the RBCs from hemolytic damage caused by a lytic agent [30]. No difference in the hemolytic activity was shown among C0, S0, and M ($P>0.05$) although Solutol HS15-based MEs had higher hemolytic activity than the CreEL-based MEs. Addition of CTAB increased the hemolytic activity. However, CTAB concentration of ≤0.4% still resulted in hemolytic activity close to negative saline control, indicating good biocompatibility. Thus, C6 and S6 were not chosen for further studies even though their hemolysis values of less than 5% was usually considered non-hemolytic.

3.5. *Protein properties*

3.5.1. *SDS-PAGE*

After 1:100 dilution, the SDS-PAGE band density in each BSA-ME lane was comparable to the one in native BSA. No aggregation and fragmentation of BSA bands were detected in either higher or lower molecular weight area. Additional bands appeared near the end of the gel were believed to be staining of wheat germ oil and/or the components of each formulation (Fig. 2A) and were also evident on the lanes of corresponding blank formulations (Fig. 2B). Moreover, the BSA bands in M and all MEs were at the same position with the BSA band in protein marker and native BSA solution (Fig. 2B) implying that the primary structure of BSA loaded in all MEs was generally conserved.

3.5.2. *Circular dichroism (CD) measurements*

The CD spectrum of native BSA solution had two negative valleys near 208 and 225 nm (Fig. 3), representing the $\pi \rightarrow \pi^*$ and $n \rightarrow \pi^*$ electron transitions [31]. The minima of BSA in all BSA-MEs slightly shifted to higher wavelengths around 209–211 nm (Fig. 3A and 3B), more likely due to changes in solvent polarity of sample [31]. Both magnitudes and shapes of CD spectra of BSA-MEs were not much different from that of

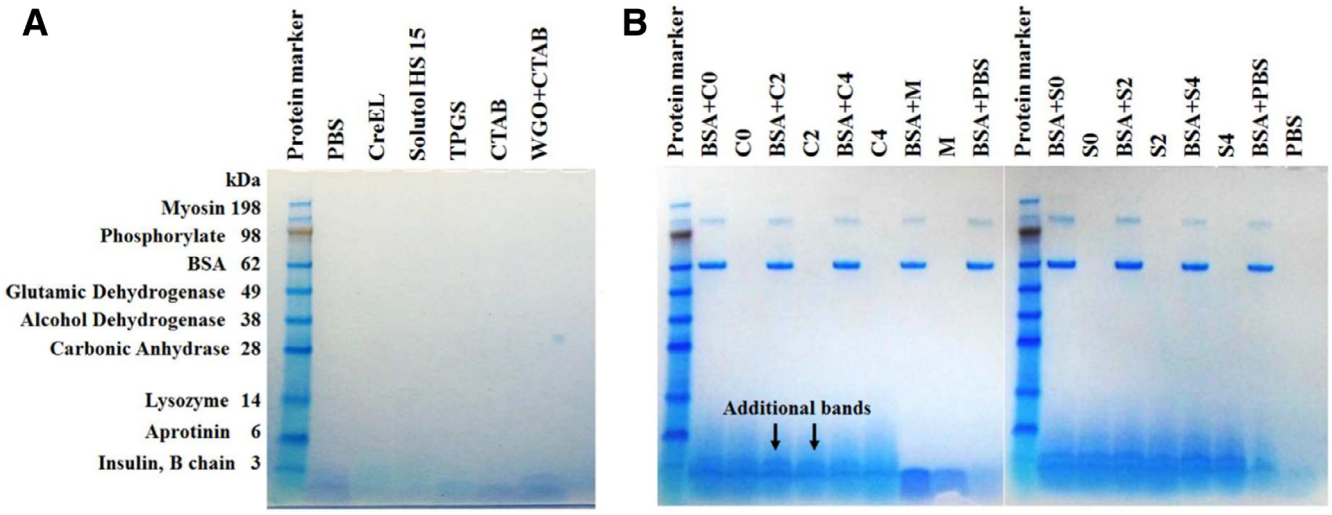

Fig. 2 – SDS-PAGE patterns of (A) ME components in PBS; (B) ME formulations showing bands of protein marker, BSA-C0, BSA-C2, BSA-C4, BSA-M, BSA-S0, BSA-S2, BSA-S4, and BSA in PBS (native BSA) compared to those of corresponding formulations without BSA, respectively. (C, S and M represent CreEL, Solutol HS15 and marketed emulsion adjuvants; the numbers, 0 2 and 4 are 0, 0.2% and 0.4% (w/v) CTAB in formulations, respectively).

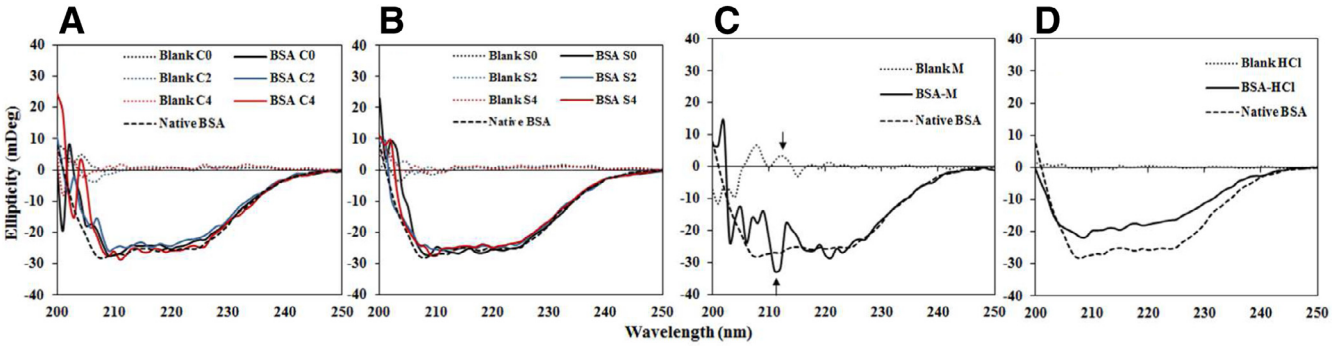

Fig. 3 – Far-UV CD spectra of (A) BSA in C0 (black line), C2 (blue line) and C4 (red line); (B) BSA in S0 (black line), S2 (blue line) and S4 (red line); (C) BSA in M and (D) BSA in 0.1 N HCl solution. (the dashed line, dotted line, and solid line refer to the spectrum of native BSA, blank formulation, and BSA in each formulation; C, S and M represent CreEL, Solutol HS15 and marketed emulsion adjuvants; the numbers, 0, 2 and 4 are 0, 0.2% and 0.4% (w/v) CTAB in formulations, respectively).

native BSA indicating no significantly conformational change of BSA in all tested MEs. In contrast, the CD spectrum of BSA-M was turbulent which was resulted from excipients used in formulations M (Fig. 3C). As a positive control, BSA degradation induced by 0.1 N hydrochloric acid (HCl) solution as positive control (Fig. 3D) exhibited less negative ellipticity values in the range 205–240 nm and decreased in native α-helical content.

3.6. *In vitro cell studies*

3.6.1. *Cell viability study*

The percentage of cell viability increased as the test volume of BSA-MEs decreased from 50 to 25 µl/well (Table 3). In contrast, BSA-M had opposite results with more than 100% cell viability from both test volumes. Low survival percentages were observed from BSA-S2 and BSA-S4 indicating high cytotoxicity, due to their greater zeta potential value. Interaction of positively charged molecules with negatively charged cell membrane would induce more pronounced disruption of cell membrane integrity which led to an increase in cytotoxicity. Thus BSA-C0, BSA-C2, BSA-C4, BSA-S0 and BSA-M at 25 µl showing more than 80 survival percentages were further assessed.

3.6.2. *Cellular uptake studies*

Quantitative analysis of cellular uptake obtained from the flow cytometry histograms of FITC-BSA loaded in MEs using 28SC cells before uptake as a baseline and present as GeoMFI data (Table 3) revealed higher cellular uptake from CreEL-based MEs than from Solutol HS15-based MEs. Moreover, C0 induced significantly higher FITC-BSA uptake than S0 ($P<0.001$) implying that CreEL could better enhance cellular uptake of incorporated proteins by human immune cells.

FITC-BSA in positively charged C2 and C4 were more taken up by 28SC cells than that in C0 ($P<0.001$). Increasing the

Table 3 – Percentages of cell viability after incubation with different volumes of BSA loaded in ME formulations and average geometric mean fluorescence intensity (GeoMFI) of 28SC cells after 2 h uptake studies of FITC-BSA loaded in ME formulations at 37 °C compared to those with M adjuvant (mean ± SD, $n = 3$).

Formulations*	Volume of sample		
	50 µl cell viability (%)	25 µl cell viability (%)	25 µl GeoMFI
Blank	–	–	2.98 ± 0.11
BSA-PBS	100.00 ± 3.20	100.00 ± 5.64	6.71 ± 0.07
BSA-C0	115.81 ± 0.80	130.50 ± 3.98	16.80 ± 0.11**
BSA-C2	83.66 ± 0.54	114.21 ± 2.86	19.80 ± 0.15**
BSA-C4	60.14 ± 1.40	86.55 ± 0.89	21.27 ± 0.13**
BSA-S0	72.56 ± 0.61	97.22 ± 1.76	11.65 ± 0.04**
BSA-S2	38.13 ± 1.42	56.20 ± 4.38	17.10 ± 2.38
BSA-S4	30.41 ± 2.43	37.66 ± 3.80	15.73 ± -
BSA-M	148.94 ± 3.25	119.27 ± 5.23	6.43 ± 0.11

* C and S represent CreEL-based MEs and Solutol HS15-based MEs and the numbers of 0, 2, 4 and 6 are 0, 0.2%, 0.4% and 0.6% (w/v) CTAB in formulations, respectively.
** $P < 0.001$, significantly different from BSA-PBS and M adjuvant.
Abbreviations: M, Marketed product.

Table 4 – Quantification of TNF-α, IL-12, and IL-10 cytokine secretion in cell supernatants promoted by the different BSA-loaded formulations (mean ± SD, $n = 3$).

Formulations*	TNF-α (pg/ml)	IL-12 (pg/ml)	IL-10 (pg/ml)
BSA-PBS	20.54 ± 0.50	0.73 ± 0.06	3.07 ± 0.09[a]
BSA-C0	30.86 ± 1.54[a,b]	0.63 ± 0.04	2.31 ± 0.14[b]
BSA-C2	28.50 ± 0.24[a,b]	0.88 ± 0.06[a,b]	2.14 ± 0.05[a,b]
BSA-C4	29.72 ± 0.58[a,b]	0.75 ± 0.04	2.21 ± 0.04[a,b]
BSA-S0	28.83 ± 0.63[a,b]	0.67 ± 0.03	2.54 ± 0.22
BSA-S2	28.43 ± 0.24[a,b]	0.69 ± 0.00	2.72 ± 0.17
BSA-S4	27.74 ± 0.56[a,b]	0.65 ± 0.02	2.71 ± 0.13
BSA-M	17.43 ± 0.30	0.71 ± 0.05	2.69 ± 0.07[b]

* C and S represent CreEL-based MEs and Solutol HS15-based MEs and the numbers of 0, 2, 4 and 6 are 0, 0.2%, 0.4% and 0.6%, w/v CTAB in formulations, respectively.
[a] $P < 0.05$, significantly different from M adjuvant.
[b] $P < 0.05$, significantly different from BSA-PBS.
Abbreviations: TNF-α, tumor necrosis factor-alpha; IL-12, interleukin-12; IL-10, interleukin-10; BSA, bovine serum albumin; M, Marketed product.

amount of cationic CTAB increased the uptake accordingly ($P<0.01$), with the GeoMFI of FITC-BSA-C2 and FITC-BSA-C4 being 19.80±0.150 and 21.27±0.132, respectively (Table 3). Similar results were observed on the uptake of PEG-oligocholic acid based micellar nanoparticles conjugated with cationic D-lysine by RAW 264.7 murine macrophages [32]. It was concluded that adjuvants consisting of positive charged components improved the uptake by cells in immune system due to electrostatic interaction between the positively charged formulations and the negatively charged plasma membranes and cell surface proteoglycan [22,24].

Considerably low uptake of FITC-BSA-M was not different from BSA alone ($P>0.05$). In addition, C0, C2, C4, and S0 significantly promoted the uptake of FITC-BSA when compared with PBS and M ($P<0.001$). Comparison to CreEL-based MEs, Solutol HS15-based MEs with greater positive surface charge surprisingly exhibited lower fluorescein uptake possibly due to higher cellular toxicity. Accordingly, histogram of FITC-BSA-S4 could not be observed. The uptake activity of immune cells predominantly relied on surface characteristics and components of adjuvant formulations.

3.6.3. *Cytokine assay*

BSA-C2 produced stronger Th1 cytokine pattern than other tested samples with significant increase in TNF-α and IL-12 levels and significant decrease in IL-10 level compared to BSA alone and BSA-M ($P<0.05$) (Table 4). The up-regulation of Th1 cytokine profile in murine macrophage cells was also noted on crosslinked chitosan nanoparticles [33]. Greater TNF-α cytokine induced by all BSA-MEs suggested a mainly responsible triggering cell-mediated immune response [34]. In CreEL-based MEs, only BSA-C2 induced an increase in IL-12 level ($P < 0.05$). Moreover, lower levels of IL-10 were observed in BSA-C0, BSA-C2, and BSA-C4 compared to BSA alone ($P < 0.05$). In addition, reduction of anti-inflammatory IL-10 production was also detected with BSA-C2 and BSA-C4 as compared to the BSA-M ($P<0.05$). No change in IL-10 and IL-12 levels by BSA-S0, BSA-S2, and BSA-S4 was noted when compared with BSA alone and BSA-M ($P>0.05$). These results indicated that the secretion level of IL-10 could be down-regulated by CreEL-based MEs especially those with cationic charges, suggesting a predominant cell-mediated immunity via inducing Th1 cytokine synthesis. Thus, formulations of C0, C2, and C4 were chosen for internalization study.

3.6.4. *Internalization study*

Confocal micrographs displayed that FITC-BSA in CreEL-based MEs were internalized and accumulated around cell membrane and nucleus of the immune cells (Fig. 4). The internalization of FITC-BSA induced by C0, C2, and C4 showed higher green intensity than that of FITC-BSA in PBS and M as shown in FITC column (white arrows in Fig. 4). Compared to C0, the surface binding and internalization of FITC-BSA in C2 and C4 seemed to enhance with regarding to increasing content of CTAB in the same manner as in the aforementioned *in vitro* cellular uptake experiment (Table 3). This result agreed with an early study on correlation of the positive surface charge of cationic nanoparticles with higher cellular uptake, faster internalization rate and further greater internalization amount [22].

In order to initiate a specific immunity to an infectious agent, the processing and presentation of antigen play a primary role in immunity. The internalization of antigens is mediated by adsorption of antigens onto the cell surface of APC and subsequent endocytosis. The processes occurring within a cell result in fragmentation of internalized proteins, association of the fragments with Major Histocompatibility Complex (MHC) molecules, and transportation of the peptide-MHC molecules to the cell surface where they can be recognized by a T-Cell. Therefore, cationic CreEL MEs may act as a highly efficient adjuvant to increase the amount of antigen which internalizes into APCs.

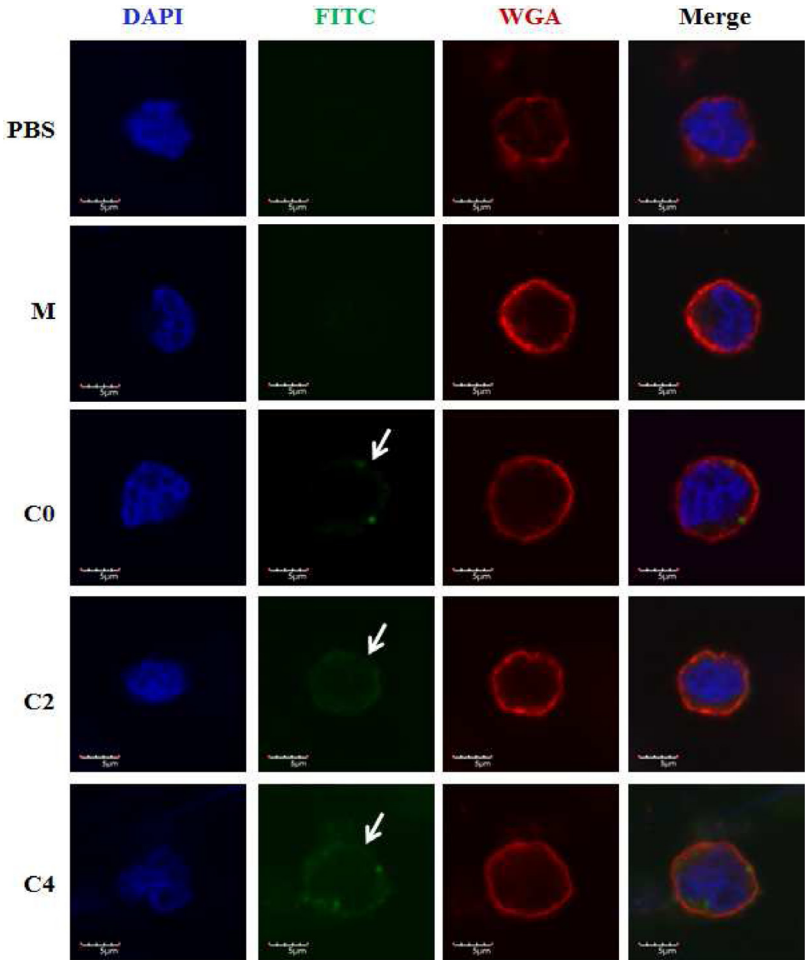

Fig. 4 – Confocal microscopy images of binding and internalization of FITC-BSA loaded in CreEL-based MEs (C0, C2, and C4) by elicited human monocyte/macrophage. FITC-BSA (green), Alexa Fluor 594-WGA (red) to label plasma membranes, DAPI (blue) to stain nuclei, and merged images represented internalization of FITC-BSA. (Scale bar in all panels equaled 5 μm and numbers of 0, 2 and 4 in formulation codes represent 0, 0.2% and 0.4% (w/v) CTAB in ME formulations, respectively.)

3.7. *Animal immunization*

3.7.1. *In vivo antibody response*

The anti-influenza (H1N1) antigen-specific total serum IgG responses after prime vaccination revealed the highest total IgG antibody titer from mice receiving Ag-M, followed by Ag-C2, and either group of Ag-C0 or Ag-C2½, with the GMT of 4673, 3125, 2556, and 2556, respectively (Fig. 5A). It was noted that both Ag-C0 and Ag-C2½ induced higher total IgG antibody responses than nonadjuvanted influenza vaccine ($P < 0.01$). As expected, the serum IgG titers of the booster vaccination exhibited higher than those of the prime vaccination ($P<0.01$) and all adjuvanted H1N1 vaccines induced higher IgG antibody titers than antigen alone ($P < 0.01$). Interestingly, similar results of total IgG titers were obtained from sera of mice vaccinated with Ag-C0 and Ag-C2½ in both prime and boost immunizations whereas the serum IgG titers of vaccinated mice with Ag-M or Ag-C2 were higher than that of mice immunized with Ag-C0 and Ag-C2½ ($P<0.05$). Furthermore, no differences in total IgG antibody responses were observed between mice immunized with Ag-M and Ag-C2 ($P>0.05$).

The IgG subtype (IgG1 and IgG2a) profiles of influenza-specific antibodies displayed that after prime vaccination, mice immunized with Ag-M showed the highest IgG1 titer of 142 858 while those immunized with Ag-C2 or Ag-C2½ showed higher IgG1 titer than their respective nonadjuvanted vaccines and Ag-C0 ($P<0.01$) (Fig. 5B and 5C). After booster dose, the serum IgG1 levels were considerably increased to 213 622, 1 953 125, 1 360 133, 1 953 125 and 1 597 198 for Ag alone, Ag-M, Ag-C0, Ag-C2, and Ag-C2½, respectively. Although IgG1 titers from both Ag-M and Ag-C2 were the highest, there were no differences in IgG1 titers among all adjuvanted groups ($P>0.05$) and all adjuvanted vaccines elicited higher serum IgG1 levels than antigen alone ($P < 0.05$).

Both Ag-M and Ag-C2 also elicited a higher production of IgG2a at 3 weeks post-prime administration than antigen alone ($P<0.01$) and Ag-C0 ($P<0.05$) (Fig. 5C). The serum IgG2a titers of mice immunized with Ag-C2½ were higher than those with Ag-alone or Ag-C0 but lower than those with

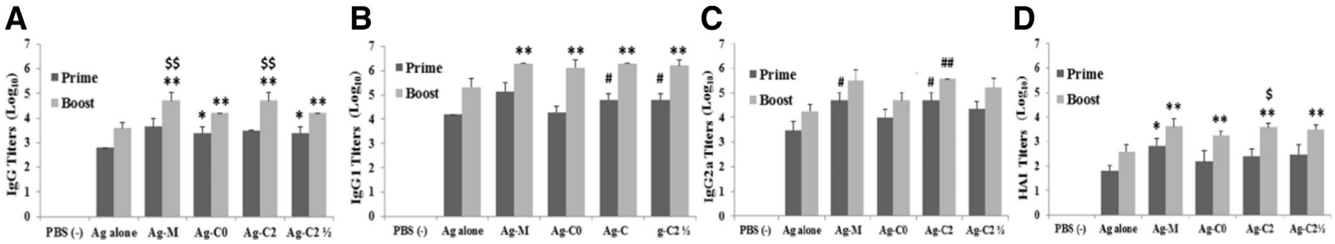

Fig. 5 – (A) Anti-influenza (H1N1) antigen-specific total serum IgG, (B) IgG1, (C) IgG2a, and (D) HAI titers in mice after the first and second intramuscular vaccination with the nonadjuvanted H1N1 vaccine (Ag alone), marketed adjuvant with vaccine (Ag-M), C0-adjuvanted vaccine (Ag-C0), C2-adjuvanted vaccine (Ag-C2), and C2-adjuvanted half-dose vaccine (Ag-C2½), respectively. (*P < 0.05 vs Ag alone (prime dose), **P < 0.05 vs Ag alone (booster dose), #P < 0.05 vs Ag alone and Ag-C0 (prime dose), ##P < 0.001 vs Ag alone and Ag-C0 (booster dose), $P < 0.05 vs C0 (booster dose), $$P < 0.05 vs Ag-C0 and Ag-C2½ (booster dose)).

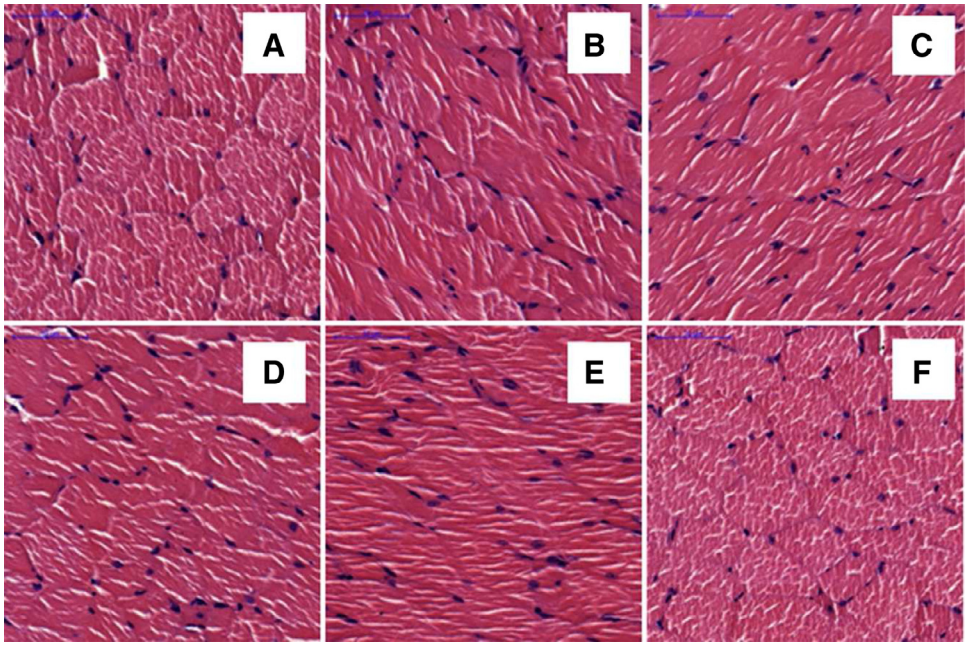

Fig. 6 – Histological photomicrographs of mice muscles injected with (A) PBS as control group, (B) antigen alone, (C) vaccine containing M adjuvant, (D) vaccine admixed with C0 adjuvant, and (E) C2 adjuvant combined with full, or (F) half-dose of antigen (C2½), respectively, and stained with hemotoxylin-eosin (H&E). (Bar in all panels equaled 50 μm.).

Ag-M or Ag-C2. However, no significant differences were observed between mice immunized with the Ag-C2½ and other adjuvanted vaccines or Ag-alone ($P>0.05$). After booster dose, the serum IgG2a levels were enhanced to 19 106, 319 440, 52 245, 390 625, and 174 693 for Ag alone, Ag-M, Ag-C0, Ag-C2, and Ag-C2½, respectively. It could be seen that only Ag-C2 could induce higher production of IgG2a in mice than antigen alone and Ag-C0 ($P<0.001$), whereas the IgG2a titers of Ag-M and Ag-C2½ did not differ from those of Ag-alone, Ag-C0, and Ag-C2 ($P>0.05$).

Both IgG1 and IgG2a antibodies are contributed to virus neutralization. The IgG1 isotype is very effective in neutralizing virus while IgG2a isotype has an important role in antibody-dependent cell-mediated immunity and provides greater protection against influenza infection by their superior ability of Fc receptor binding on macrophage or complement activating [35]. Thus, the potential induction of serum IgG1 and IgG2a responses would increase vaccine efficacy against viral infections.

3.7.2. *Hemagglutination inhibition titers*

Results of HAI titers confirmed the results of ELISA titers due to relation between HAI titer and IgG1 and IgG2a levels. There was no detectable HAI titer for the group of mice immunized with the PBS as a negative control (Fig. 5D). After prime vaccination, HAI titer in the Ag-M was higher than that of nonadjuvanted group ($P<0.05$). After booster dose, higher HAI titers were elicited by all adjuvanted vaccines than by antigen alone ($P<0.05$). In addition, HAI titer showed no difference between Ag-MEs and Ag-M group ($P>0.05$). Consistence with the antibody responses, HAI titers from Ag-C0 were lower than that of Ag-C2 after second vaccination ($P<0.05$).

The vaccine administration with Ag-C0 could induce higher total serum IgG in the first and second vaccination as well as IgG1 and HAI titers after the second booster compared to the nonadjuvanted vaccine. These results were consistent with the *in vitro* study on the enhancement of cellular uptake and internalization of incorporated FITC-BSA by 28SC cells including the greater levels of TNF-α cytokine production and the significant down-regulation of IL-10 in human immune cells compared to BSA alone, suggesting a dominant Th1 cytokine synthesis to facilitate elimination of influenza infection [34]. Moreover, stronger immune response and better effectiveness following vaccination from Ag-C0 than from the antigen alone implying the possible immunogenic effects of uncharged adjuvant compositions, likely due to synergistic effect with high vitamin E content in wheat germ oil and TPGS which could enhance the antigen uptake [19] and antibody responses [19,20].

The C0 and C2 illustrated the properties of formulation composition-dependent immunogenicity. The adjuvant effects of cationic surfactant in C2 obviously showed better immune responses than antigen alone and C0 vaccine. C2 enhanced higher FITC-BSA uptake and greater FITC-BSA internalization than antigen alone, C0 and M, in addition to the promotion of Th1 type cytokines both IL-12 and TNF-α and a mixed Th1/Th2-type profile, with a trend for higher IgG2a antibody response which could lead to significant protection from lethal influenza virus challenge.

Interestingly, C2 induced dose sparing while retaining immunogenicity. The significantly stronger levels of total IgG, IgG1 and HAI titers were achieved with a half dose of influenza vaccine using C2 compared to a full dose of vaccine alone ($P<0.05$). Moreover, C2 with half-dose antigen (Ag-C2½) was superior to C0 with full-dose antigen (Ag-C0) in terms of the magnitude of immune responses, resulting in an enhancement in IgG1 antibody responses after the first immunization ($P<0.05$). After prime and boost immunizations, there were no differences in IgG1, IgG2a and HAI titers between mice receiving Ag-C2½ and Ag-M or Ag-C2 ($P>0.05$). The capacity of adjuvant to allow similar responses with lower amounts of antigen required in vaccines would be beneficial in situations in which large-scale vaccine production is urgent as in the emergence of a pandemic influenza strain.

According to these results, the prepared MEs both C0 and C2 formulations had the potential to be novel adjuvants for parenteral vaccine administration. These efficiencies were clearly more pronounced from C2, which was capable of antigen dose sparing without the concomitant loss of immune response.

3.7.3. *Histomicroscopic examinations*

Myocytes seen in cross section revealed purple-blue nuclei located at the periphery of individual myofiber with red-pink sarcoplasm (Fig. 6). All histomicroscopic images of muscle biopsy specimens demonstrated homogenous myofiber size distribution, and polygonal shaped muscle fibers without many inflammatory cells indicating normal histological features. None of the formulations induced inflammatory changes or necrosis areas with no evidence of degeneration. No alterations were observed in muscle cells from the adjuvanted groups (Fig. 6C-F) compared to those with PBS (Fig. 6A) and antigen alone (Fig. 6B). Thus, it could be inferred that C0, C2 and M were safe to muscles at the injection site.

4. Conclusion

In conclusion, the developed cationic MEs showed good physical stability, autoclaving capacity, and biocompatibility and improved the uptake of model antigen to immune cells. Animals immunized with cationic ME vaccines significantly increased the humoral and cellular immune response against split H1N1 influenza virus compared with the nonadjuvanted vaccine. No significant differences in immune responses were observed between mice immunized with the marketed O/W emulsion adjuvant and the selected cationic CreEL-based ME adjuvant (C2). Therefore, the cationic MEs had potential to act as a novel adjuvant for parenteral vaccine administration.

Conflicts of interest

The authors report no conflicts of interest. The authors alone are responsible for the content and writing of this article.

Acknowledgments

Research grant from the Office of Higher Education Commission via Chulalongkorn University, the fiscal year 2014–2015 is acknowledged. The authors gratefully acknowledge Government Pharmaceutical Organization (Bangkok, Thailand) for kindly providing influenza vaccine and also thank the Thai Red Cross Society for kind support on human blood. Appreciation is to Noppadol Sa-Ard-Iam (Unit Cell of Immunopathological/Clinical Research in Periodontal Disease, Faculty of Dentistry, Chulalongkorn University) for FACS flow cytometry study. Thanks to the staff at Olympus Bioimaging Center, Faculty of Science, Mahidol University for their technical help and use of their microscope facility.

Supplementary material

Supplementary material associated with this article can be found, in the online version, at doi:10.1016/j.ajps.2019.08.002.

REFERENCES

[1] Ahmed SS, Schur PH, MacDonald NE, Steinman L. Narcolepsy, 2009 A(H1N1) pandemic influenza, and pandemic influenza vaccinations: what is known and unknown about the neurological disorder, the role for autoimmunity, and vaccine adjuvants. J Autoimmun 2014;50:1–11.

[2] Oda K, Tsukahara F, Kubota S, Kida K, Kitajima T, Hashimoto S. Emulsifier content and side effects of oil-based adjuvant vaccine in swine. Res Vet Sci 2006;81:51–7.

[3] Miyaki C, Quintilio W, Miyaji EN, Botosso VF, Kubrusly FS, Santos FL, et al. Production of H5N1 (NIBRG-14) inactivated

whole virus and split virion influenza vaccines and analysis of immunogenicity in mice using different adjuvant formulations. Vaccine 2010;28:2505–9.
[4] Alves RCB, New RRC, Andrade GR, Mendonça RMZ, Sant'Anna OABE, Mancini DAP, et al. Vaxcine (TM): an oil-based adjuvant for influenza vaccines. Mem Inst Oswaldo Cruz 2011;106:1052–4.
[5] Hamouda T, Sutcliffe JA, Ciotti S, Baker JR Jr. Intranasal immunization of ferrets with commercial trivalent influenza vaccines formulated in a nanoemulsion-based adjuvant. Clin Vaccine Immunol 2011;18:1167–75.
[6] Deng JH, Cai WH, Jin F. A novel oil-in-water emulsion as a potential adjuvant for influenza vaccine: development, characterization, stability and *in vivo* evaluation. Int J Pharm 2014;468:187–95.
[7] Galliher-Beckley A, Pappan LK, Madera R, Burakova Y, Waters A, Nickles M, et al. Characterization of a novel oil-in-water emulsion adjuvant for swine influenza virus and mycoplasma hyopneumoniae vaccines. Vaccine 2015;33:2903–8.
[8] Jain J, Fernandes C, Patravale V. Formulation development of parenteral phospholipid-based microemulsion of etoposide. AAPS PharmSciTech 2010;11:826–31.
[9] Fan YP, Ma L, Zhang WM, Xu YY, Zhi XY, Cui EH, et al. Microemulsion can improve the immune-enhancing activity of propolis flavonoid on immunosuppression and immune response. Int J Biol Macromol 2014;63:126–32.
[10] Lee JJ, Shim A, Lee SY, Kwon BE, Kim SR, Ko HJ, et al. Ready-to-use colloidal adjuvant systems for intranasal immunization. J Colloid Interface Sci 2016;467:121–8.
[11] Leclercq SY, dos Santos RM, Macedo LB, Campos PC, Ferreira TC, de Almeida JG, et al. Evaluation of water-in-oil-in-water multiple emulsion and microemulsion as potential adjuvants for immunization with rabies antigen. Eur J Pharm Sci 2011;43:378–85.
[12] Macedo LB, Lobato ZIP, Fialho SL, Viott ADM, Guedes RMC, Silva-Cunha A. Evaluation of different adjuvants formulations for bluetongue vaccine. Braz Arch Biol Technol 2013;56:932–41.
[13] Jiang W, Kim BY, Rutka JT, Chan WC. Nanoparticle-mediated cellular response is size-dependent. Nat Nanotechnol. 2008;3:145–50.
[14] Reddy ST, Rehor A, Schmoekel HG, Hubbell JA, Swartz MA. *In vivo* targeting of dendritic cells in lymph nodes with poly(propylene sulfide) nanoparticles. J Control Release 2006;112:26–34.
[15] Biesalski HK. Vitamin e requirements in parenteral nutrition. Gastroenterology 2009;137:S92–104.
[16] Gumus ZP, Guler E, Demir B, Barlas FB, Yavuz M, Colpankan D, et al. Herbal infusions of black seed and wheat germ oil: their chemical profiles, *in vitro* bio-investigations and effective formulations as phyto-nanoemulsions. Colloids Surf B Biointerfaces 2015;133:73–80.
[17] Weiguo F., Wei W. and Peixian W. Cinobufagin emulsion for injection and its prepn process. CN1846712A. 2006.
[18] Stone HD. Newcastle disease oil emulsion vaccines prepared with animal, vegetable, and synthetic oils. Avian Dis 1997;41:591–7.
[19] Vervarcke S, Ollevier F, Kinget R, Michoel A. Oral vaccination of african catfish with vibrio anguillarum O2: effect on antigen uptake and immune response by absorption enhancers in lag time coated pellets. Fish Shellfish Immunol 2004;16:407–14.
[20] Somavarapu S, Pandit S, Gradassi G, Bandera M, Ravichandran E, Alpar OH. Effect of vitamin E TPGS on immune response to nasally delivered diphtheria toxoid loaded poly(caprolactone) microparticles. Int J Pharm 2005;298:344–7.
[21] Allen TM, Austin GA, Chonn A, Lin L, Lee KC. Uptake of liposomes by cultured mouse bone marrow macrophages: influence of liposome composition and size. Biochim Biophys Acta 1991;1061:56–64.
[22] Yue ZG, Wei W, Lv PP, Yue H, Wang LY, Su ZG, et al. Surface charge affects cellular uptake and intracellular trafficking of chitosan-based nanoparticles. Biomacromolecules 2011;12:2440–6.
[23] Denis-Mize KS, Dupuis M, MacKichan ML, Singh M, Doe B, O'Hagan D, et al. Plasmid dna adsorbed onto cationic microparticles mediates target gene expression and antigen presentation by dendritic cells. Gene Ther 2000;7:2105–12.
[24] Saini V, Jain V, Sudheesh MS, Jaganathan KS, Murthy PK, Kohli DV. Comparison of humoral and cell-mediated immune responses to cationic plga microspheres containing recombinant hepatitis b antigen. Int J Pharm 2011;408:50–7.
[25] Fox CB, Lin S, Sivananthan SJ, Dutill TS, Forseth KT, Reed SG, et al. Effects of emulsifier concentration, composition, and order of addition in squalene-phosphatidylcholine oil-in-water emulsions. Pharmaceut Dev Tech 2011;16:511–19.
[26] World Health Organization. WHO manual on animal influenza diagnosis and surveillance. 2002. Available from: http://www.who.int/csr/resources/publications/influenza/en/whocdscsrncs20025rev.pdf. [accessed Febuary 12, 2016].
[27] Jumaa M, Müller BW. Physicochemical properties of chitosan-lipid emulsions and their stability during the autoclaving process. Int J Pharm 1999;183:175–84.
[28] Rowe RC, Sheskey PJ, Quinn ME, editors. Handbook of pharmaceutical excipients. 6th ed. London; Chicago; Washington, DC: Pharmaceutical Press and American Pharmacists Association; 2009.
[29] Ohnishi M, Sagitani H. The effect of nonionic surfactant structure on hemolysis. J Am Oil Chem' Soc 1993;70:679–84.
[30] Jumaa M, Müller BW. Lipid emulsions as a novel system to reduce the hemolytic activity of lytic agents: mechanism of the protective effect. Eur J Pharm Sci 2000;9:285–90.
[31] Miles AJ, Wallace BA. Circular dichroism spectroscopy of membrane proteins. Chem Soc Rev 2016;45:4859–72.
[32] Xiao K, Li Y, Luo J, Lee JS, Xiao W, Gonik AM, et al. The effect of surface charge on *in vivo* biodistribution of PEG-oligocholic acid based micellar nanoparticles. Biomaterials 2011;32:3435–46.
[33] Yue H, Wei W, Yue Z, Lv P, Wang L, Ma G, et al. Particle size affects the cellular response in macrophages. Eur J Pharm Sci 2010;41:650–7.
[34] Gandhi GR, Neta MTSL, Sathiyabama RG, Quintans JdSS, de Oliveira e Silva AM, Araújo AAdS, et al. Flavonoids as Th1/Th2 cytokines immunomodulators: a systematic review of studies on animal models. Phytomedicine 2018;44:74–84.
[35] Unkeless JC, Eisen HN. Binding of monomeric immunoglobulins to fc receptors of mouse macrophages. J Exp Med 1975;142:1520–33.